

1 **Fluorarrojadite-(BaNa), BaNa<sub>4</sub>CaFe<sub>13</sub>Al(PO<sub>4</sub>)<sub>11</sub>(PO<sub>3</sub>OH)F<sub>2</sub>, a new member**  
2 **of the arrojadite group from Gemerská Poloma, Slovakia**

3 MARTIN ŠTEVKO<sup>1\*</sup>, JIŘÍ SEJKORA<sup>2</sup>, PAVEL UHER<sup>3</sup>, FERNANDO CÁMARA<sup>4</sup>, RADEK  
4 ŠKODA<sup>5</sup> and TOMÁŠ VACULOVIČ<sup>6</sup>

5  
6 <sup>1</sup> Pribišova 15, 841 05 Bratislava, Slovak Republic

7 <sup>2</sup> Department of Mineralogy and Petrology, National Museum, Cirkusová 1740, 193 00  
8 Prague 9 - Horní Počernice, Czech Republic

9 <sup>3</sup> Department of Mineralogy and Petrology, Faculty of Natural Sciences, Comenius  
10 University, Ilkovičova 6, 842 15 Bratislava, Slovak Republic

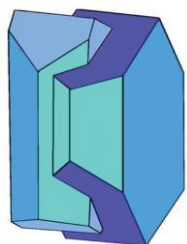
11 <sup>4</sup> Dipartimento di Scienze della Terra "A. Desio", Università di Milano, via Mangiagalli 34,  
12 20133 Milano, Italy

13 <sup>5</sup> Department of Geological Sciences, Faculty of Science, Masaryk University, Kotlářská 2,  
14 611 37 Brno, Czech Republic

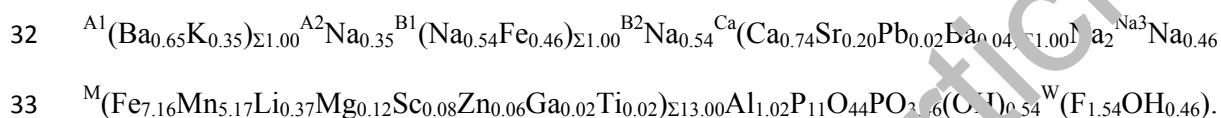
15 <sup>6</sup> Department of Chemistry, Faculty of Science, Masaryk University, Kotlářská 2, 611 37  
16 Brno, Czech Republic

17  
18 \* Corresponding author, e-mail: msminerals@gmail.com

19  
20 **Abstract:** The new mineral fluorarrojadite-(BaNa), ideally BaNa<sub>4</sub>CaFe<sub>13</sub>Al(PO<sub>4</sub>)<sub>11</sub>(PO<sub>3</sub>OH)F<sub>2</sub>  
21 was found on the dump of of Elisabeth adit near Gemerská Poloma, Slovakia. It occurs in  
22 hydrothermal quartz veins intersecting highly fractionated, topaz-zinnwaldite S-type  
23 leucogranite. Fluorarrojadite-(BaNa) is associated with fluorapatite, “fluordickinsonite-  
24 (BaNa)”, triplite, viitaniemiite and minor amounts of other minerals. It forms fine grained



25 irregular aggregates up to 4 x 2 cm, which consists of individual anhedral grains up to 0.01  
26 mm in size. It has a yellowish-brown to greenish-yellow colour, very pale yellow streak, a  
27 vitreous to greasy lustre. Mohs hardness is about 4½ to 5. The fracture is irregular and the  
28 tenacity is brittle. The measured density is 3.61(2) g·cm<sup>-3</sup> and calculated density is 3.650  
29 g·cm<sup>-3</sup>. Fluorarrojadite-(BaNa) is biaxial (+) and nonpleochroic. The calculated refractive  
30 index based on empirical formula is 1.674. The empirical formula (based on 47 O and 3  
31 (OH+F) *apfu*) is



34 Fluorarrojadite-(BaNa) is monoclinic, space group *Cc*,  $a = 16.553(1)$  Å,  $b = 10.0476(6)$  Å,  $c =$   
35  $24.669(1)$  Å,  $\beta = 105.452(4)^\circ$ ,  $V = 3957.5(4)$  Å<sup>3</sup> and  $Z = 4$ . The seven strongest reflections in  
36 the powder X-ray diffraction pattern are [ $d_{\text{obs}}$  in Å, ( $h, k, l$ ): 3.412, (21), 116; 3.224, (37), 206;  
37 3.040, (100), 42-4; 2.8499, (22), 33-2; 2.7135, (56), 22-3; 2.5563, (33), 028 and 424; 2.5117,  
38 (23), 040. The new mineral is named according to the actual nomenclature scheme of  
39 arrojadite group minerals, which was approved by the CNMNC IMA. In fluorarrojadite-  
40 (BaNa) Fe<sup>2+</sup> is a dominant cation at the M site (so the root-name is arrojadite) and two  
41 suffixes are added to the root-name according to the dominant cation of the dominant valence  
42 state at the A1 (Ba<sup>2+</sup>) and B1 sites (Na<sup>+</sup>). A prefix fluor is added to the root-name as F<sup>-</sup> is  
43 dominant over (OH) at the W site.

44 **Key-words:** fluorarrojadite-(BaNa); new mineral; arrojadite group; phosphates; Raman  
45 spectroscopy; S-type granite; Gemerská Poloma; Slovakia

46 **Running title:** Fluorarrojadite-(BaNa), a new member of arrojadite group

47

## 48 **Introduction**

49 Fluorarrojadite-(BaNa), ideally  $\text{BaNa}_4\text{CaFe}_{13}\text{Al}(\text{PO}_4)_{11}(\text{PO}_3\text{OH})\text{F}_2$  is a new member of  
50 arrojadite group. It was found at the dump of Elisabeth adit near Gemerská Poloma village,  
51 Rožňava Co., Košice Region, Slovak Republic.

52 The new mineral is named according to actual nomenclature scheme of arrojadite  
53 group minerals (Chopin *et al.*, 2006), which was approved by the CNMNC IMA and it is  
54 based on the occupancy of M (root-name), A1 (first suffix), B1 (second suffix) and W (first  
55 prefix) sites. Three root-names are recognized for arrojadite group minerals: arrojadite ( $\text{Fe}^{2+}$   
56 dominant at M sites), dickinsonite ( $\text{Mn}^{2+}$  dominant at M sites) and carnoite (Mg dominant at  
57 the M sites; successively found and approved by the CNMNC IMA, Cámara *et al.*, 2015).

58 General structural formula for arrojadite group mineral is  
59  $\text{A}_2\text{B}_2\text{CaNa}_{2+x}\text{M}_{13}\text{Al}(\text{PO}_4)_{11}(\text{PO}_3\text{OH}_{1-x})\text{W}_2$  (for details see Chopin *et al.*, 2006). In  
60 fluorarrojadite-(BaNa)  $\text{Fe}^{2+}$  is dominant cation at the M site (so the root-name is arrojadite)  
61 and two suffixes are added to the root-name according to the dominant cation of the dominant  
62 valence state at the A1 ( $\text{Ba}^{2+}$ ) and B1 sites ( $\text{Na}^+$ ). Prefix fluor is added to the root-name as F  
63 is dominant over  $(\text{OH})^-$  at the W site.

64 The new mineral and the name were approved by the Commission on New Minerals,  
65 Nomenclature and Classification of the International Mineralogical Association (IMA 2016-  
66 075). The description of fluorarrojadite-(BaNa) is based upon two holotype specimens (two  
67 parts of one large piece). One is deposited in the collections of the Department of Mineralogy  
68 and Petrology, National Museum in Prague, Cirkusová 1740, 19300 Praha 9, Czech Republic  
69 under the catalogue number P1P 13/2016. The second holotype specimen is deposited in the  
70 collections of the Department of Mineralogy and Petrology, Faculty of Natural Sciences,  
71 Comenius University, Ilkovičova 6, 84215 Bratislava IV, Slovak Republic under the  
72 catalogue number 7401.

73 **Occurrence**

74 Several specimens with fluorarrojadite-(BaNa) were found at the dumps of Elisabeth  
75 adit (which exploited Gemerská Poloma talc deposit) situated near Gemerská Poloma village,  
76 Rožňava Co., Košice Region, Slovak Republic (48°45'04.06" N, 20°29'39.27" E). During the  
77 exploration of the talc-magnesite deposit main crosscut of Elisabeth adit intersected large  
78 body of specialized S-type granite (also called Gemic granite) with the abundant  
79 hydrothermal quartz veins containing fluorarrojadite-(BaNa).

80 The granitic rocks of the Gemic Unit represent a distinct type of specialized (Sn-W-  
81 F), highly evolved suite with S-type affinity, which differs from other granitoids occurring in  
82 the Veporic and Tatric Units of the Western Carpathian crystalline basement; they are  
83 enriched in phosphorus and rare lithophile elements, such as Li, Rb, Cs, B, Ga, Sn, W, Nb,  
84 Ta, U and depleted in REE, Zr, Ti, Sr, Ba (e.g., Uher and Broska, 1996; Petrik and Kohút,  
85 1997; Kubiš and Broska, 2005; Kubiš and Broska, 2010; Breiter *et al.*, 2015). The Gemic  
86 granitic rocks forms several small plutons intruded to the intensively folded Lower Paleozoic  
87 (mainly Ordovician to Devonian) volcano-sedimentary complex of the Gelnica Group,  
88 metamorphosed in the greenschist metamorphic facies (Bajaník *et al.*, 1984; Petrasová *et al.*,  
89 2007). In the Gemerská Poloma area, the metamorphic rocks are composed mainly of  
90 phyllites, metayoung volcanic rocks of rhyolitic to dacitic composition, locally with lenses of  
91 metabasites and strongly steatitized magnesite with recently exploited talc deposit near  
92 Gemerská Poloma (Kilík, 1997). The age of granite intrusion and related hydrothermal veins  
93 with fluorarrojadite-(BaNa) and other phosphates is Late Permian (~260 to 250 Ma), on the  
94 basis of zircon U-Pb dating of the granites (Poller *et al.*, 2002) and Re-Os molybdenite dating  
95 of related Sn-W-Mo mineralization (Kohút and Stein, 2005).

96 Several types of the Gemic granites were distinguished at the Gemerská Poloma  
97 area: **(a)** coarse-grained porphyritic granite to granite porphyry, **(b)** medium-grained Li-

98 annite-topaz-tourmaline bearing granite, (c) P-enriched topaz-zinnwaldite leucogranite and  
99 (d) albitite (Dianiška *et al.*, 2002; Dianiška *et al.*, 2007; Petřík *et al.*, 2014; Breiter *et al.*,  
100 2015). Except of albitites, all listed types of granite were recently encountered in the Elisabeth  
101 adit (Števkó *et al.*, 2015).

102 The hydrothermal quartz veins with albite, muscovite, fluorite, siderite, calcite,  
103 dolomite, sulphides and sulphosalts were observed in all types of granite, but the occurrence  
104 of the quartz veins with fluorarrodite-(BaNa) and other phosphates  
105 (fluorapatite, “fluordickinsonite-(BaNa)”, triplite and viitaniemiite) is limited only to the  
106 highly fractionated topaz-zinnwaldite leucogranite (Števkó *et al.*, 2016). The quartz veins  
107 with fluorarrodite-(BaNa) are up to 8 cm thick and no more than 1 m long and except of  
108 other phosphates (common and macroscopic: fluorapatite and triplite; rare and microscopic:  
109 viitaniemiite; very rare and microscopic: “fluordickinsonite-(BaNa)”) they contain minor  
110 amounts of albite, orthoclase, muscovite, fluorite, iron-rich siderite to rhodochrosite,  
111 arsenopyrite, pyrite, bismuthinite, kobeinite, tininite, giessenite and native bismuth.

## 112 **Physical and optical properties**

113 Fluorarrodite-(BaNa) occurs as very fine grained irregular aggregates usually up to 1  
114 x 1 cm in size, exceptionally up to 4 x 2 cm (Figure 1), which consists of individual anhedral  
115 grains up to 0.01 mm. Individual crystals have not been observed. It has a yellowish-brown to  
116 greenish-yellow colour, very pale yellow streak, a vitreous to greasy lustre and is non-  
117 fluorescent in SW and LW ultraviolet light. The Mohs hardness is estimated at about 4½ to 5  
118 based upon scratch tests and by analogy to other arrojadite group minerals. The fracture is  
119 irregular and tenacity is brittle. No cleavage was observed as aggregates of fluorarrodite-  
120 (BaNa) are fine grained. The measured density acquired by floating of the mineral fragments  
121 in a mixture of the Clerici solution (density 4.2 g·cm<sup>-3</sup>) and distilled water is 3.61(2) g·cm<sup>-3</sup>,  
122 whereas calculated density is 3.650 g·cm<sup>-3</sup> based on the empirical formula and unit-cell

123 volume. Fluorarrojadite-(BaNa) is optically biaxial (+) without apparent pleochroism.  
124 Refractive indexes and other optical properties were not determined due to very small single  
125 grain size. The calculated refractive index based on the empirical formula is 1.674.

126

### 127 **Raman spectroscopy**

128 Raman spectrum of fluorarrojadite-(BaNa) was collected in the range 3580-50 cm<sup>-1</sup>  
129 using a DXR dispersive Raman Spectrometer (Thermo Scientific) mounted on a corocal  
130 Olympus microscope at the Department of Mineralogy and Petrology, National Museum,  
131 Prague, Czech Republic. The Raman signal was excited by a green 532 nm diode-pumped  
132 solid-state laser and detected by a CCD detector. The experimental parameters were: 10x  
133 objective, 1 s exposure time, 1000 exposures, 900 lines/mm grating, 50 µm slit spectrograph  
134 aperture and 8 mW laser power level. The instrument was set up by a software-controlled  
135 calibration procedure using multiple neon emission lines (wavelength calibration), multiple  
136 polystyrene Raman bands (laser frequency calibration) and standardized white-light sources  
137 (intensity calibration). Spectral manipulations were performed using the Omnic 9 software  
138 (Thermo Scientific).

139 Raman spectrum (Figure 2a-c) of fluorarrojadite-(BaNa) is similar to spectra published  
140 by Frost *et al.* (2013) for arrojadite-(KFe) as same as to those from RRUFF database  
141 ([www.rruff.info](http://www.rruff.info); Lafuente *et al.* 2015) - arrojadite-(KNa) (R050107), arrojadite-(KFe)  
142 (R070317) and arrojadite-(NaFe) (R-070298). The existence of several non-equivalent (PO<sub>4</sub>)<sup>3-</sup>  
143 groups, their strong distortion and presence of (PO<sub>3</sub>OH)<sup>2-</sup> group in the crystal structure of  
144 proposed new mineral lead to complex Raman spectrum with a lot of overlapping bands  
145 corresponding to stretching and bending vibrations of phosphate groups (Nakamoto, 1986).  
146 The most intensive bands in the region 1060 - 830 cm<sup>-1</sup> (1020, 985, 959, 939, 916 and 839  
147 cm<sup>-1</sup>) corresponds to ν<sub>1</sub> symmetric stretching vibration of (PO<sub>4</sub>)<sup>3-</sup> and (PO<sub>3</sub>OH)<sup>2-</sup> groups; those

148 at 1151, 1113 and 1076  $\text{cm}^{-1}$  to  $\nu_3$  antisymmetric stretching vibration of  $(\text{PO}_4)^{3-}$  and  
149  $(\text{PO}_3\text{OH})^{2-}$  groups. The bending vibrations of  $(\text{PO}_4)^{3-}$  and  $(\text{PO}_3\text{OH})^{2-}$  groups are represented  
150 by bands in the region with frequencies between 700 and 400  $\text{cm}^{-1}$ : 507, 481, 461, 439 and  
151 414  $\text{cm}^{-1}$  ( $\nu_2$ ) and 643, 602, 580, 575, 551 and 532  $\text{cm}^{-1}$  ( $\nu_4$ ). The observed bands at 3551 and  
152 3523  $\text{cm}^{-1}$  are connected to stretching vibrations of OH groups. These compare well with  
153 stretching vibrations observed by Cámara *et al.* (2006) in Nickel Plate mine arrojadite-(KFe)  
154 and Rapid Creek arrojadite-(KNa) and also with FTIR absorbance data by Della Ventura *et al.*  
155 (2014) for Nickel Plate mine arrojadite-(KFe). Note, the absence of molecular water in the  
156 studied mineral phase is confirmed by no observed bands in the area 1650–1550  $\text{cm}^{-1}$ .

### 157 **Chemical composition**

158 Quantitative chemical analyses (5 points) of fluorarrojadite-(BaNa) were performed at  
159 the Laboratory of Electron Microscopy and Microanalysis of the Masaryk University and  
160 Czech Geological Survey in Brno, Czech Republic on the Cameca SX100 electron  
161 microprobe equipped with five wavelength-dispersive spectrometers. Analytical conditions  
162 were following: 15 kV accelerating voltage, 10 nA beam current, 10  $\mu\text{m}$  beam diameter and  
163 WDS mode. Raw X-ray intensities were corrected for matrix effects with a  $\phi(\rho z)$  algorithm  
164 (Pouchou and Pichot, 1991).

165 The contents of trace elements in fluorarrojadite-(BaNa) were determined by LA-ICP-  
166 MS at Department of Chemistry, Faculty of Science, Masaryk University, Brno, Czech  
167 Republic. The setup consists of laser ablation system UP213 (New Wave, USA) and  
168 quadrupole ICP-MS Agilent 7500ce (Agilent Technologies, Japan). Ablation system is  
169 equipped with Nd:YAG laser emitting radiation with wavelength of 213 nm. Laser ablation  
170 was performed with a single hole drilling mode for the duration of 60 seconds for each spot of  
171 100  $\mu\text{m}$  diameter, laser fluency of 12  $\text{J cm}^{-2}$ , and repetition rate of 10 Hz. The LA-ICP-MS  
172 measurements were normalized on average electron-microprobe measured concentration of

173 phosphorus in fluorarrojadite-(BaNa) and the NIST SRM 610 glass reference material was  
174 used. Analytical data for fluorarrojadite-(BaNa) as well as standards used are given in **Table 1**  
175 and the LA-ICP-MS analyses of selected trace elements in fluorarrojadite-(BaNa) are given in  
176 **Table 2**.

177 The average composition of fluorarrojadite-(BaNa) corresponds to the empirical  
178 formula (based on  $47 \text{ O OH} + \text{F} = 2 + [21 - \text{the sum of non-(P,Al) cations}] \text{ apfu}$ , Chopin *et al.*  
179 2006):

180  $(\text{Na}_{3.96}\text{Ca}_{0.74}\text{Ba}_{0.69}\text{K}_{0.35}\text{Sr}_{0.20}\text{Pb}_{0.02})_{\Sigma 5.96}^{\text{M}}(\text{Fe}_{7.62}\text{Mn}_{5.17}\text{Li}_{0.37}\text{Mg}_{0.12}\text{Sc}_{0.08}\text{Zn}_{0.06}\text{Ti}_{0.02}\text{Ga}_{0.02})_{\Sigma 13.46}\text{Al}$   
181  $_{1.02}(\text{P}_{12.02}\text{O}_{47})(\text{F}_{1.54}\text{OH}_{1.00}\text{O}_{0.46})_{\Sigma 3.00}$ . The elements have been grouped into four categories:  
182 large low-charge cations (alkali and alkaline earth metals plus lead occupying high  
183 coordination number sites; small alkali and alkaline earth metals plus transition metals in  
184 four-, five- and six-fold coordinated sites; Al (Ga) in small octahedra and P in tetrahedral  
185 coordination. The sum of  $[\text{Fe}+\text{Mn}+\text{Mg}+\text{Li}+(\text{Sc}, \text{Zn}, \text{Ti})] > 13 \text{ apfu}$ , but it is  $< 13.5$  therefore  
186 precluding dominance of Fe (or Mn) in the B1 oct sites described by Chopin *et al.* (2006). In  
187 addition, the sum of alkali and alkaline earth metals close to  $6 \text{ apfu}$ , out of them 1.69 are  
188 divalent cations (essentially Ca and Ba), and this implies that the formula scheme has to be  
189 no. 3 in Table 3 of Chopin *et al.* (2006). Therefore, Ba must be dominant at A1 site and Na at  
190 B1 site. Furthermore, the analysed fluorine content is  $\text{F} > 1.5 \text{ apfu}$ , distinguishing it from the  
191 composition reported by Vignola *et al.* (2015), and thus this mineral has to be classified as  
192 fluorarrojadite-(BaNa).

193 In absence of site partitioning that can be obtained only from crystal structure  
194 refinement (see below), site assignment follows the cation ordering scheme proposed by  
195 Cámara *et al.* (2006), allow to guess the ordering of the cations in the different sites of the  
196 structure, thus leading to the following crystal-chemical formula:

197  $^{\text{A1}}(\text{Ba}_{0.65}\text{K}_{0.35})_{\Sigma 1.00}^{\text{A2}}\text{Na}_{0.35}^{\text{B1}}(\text{Na}_{0.54}\text{Fe}_{0.46})_{\Sigma 1.00}^{\text{B2}}\text{Na}_{0.54}^{\text{Ca}}(\text{Ca}_{0.74}\text{Sr}_{0.20}\text{Pb}_{0.02}\text{Ba}_{0.04})_{\Sigma 1.00}\text{Na}_2^{\text{Na3}}\text{Na}_{0.46}$



198  $M(\text{Fe}_{7.16}\text{Mn}_{5.17}\text{Li}_{0.37}\text{Mg}_{0.12}\text{Sc}_{0.08}\text{Zn}_{0.06}\text{Ga}_{0.02}\text{Ti}_{0.02})_{\Sigma 13.00}\text{Al}_{1.02}\text{P}_{11}\text{O}_{44}\text{PO}_{3.46}(\text{OH})_{0.54}^W(\text{F}_{1.54}\text{OH}_{0.46})$   
 199  $\Sigma 2.00$ . The presence of 0.46 *apfu* of  $\text{Fe}^{2+}$  at B1 sites implies that B2 can be at most occupied by  
 200 0.56 *apfu* of Na, the remaining Na occupying partially the Na3 site. This implies that in the  
 201 calculation of total amount of (F+OH), the Na present at Na3 site must be subtracted to 3  
 202 (F+OH), because the occupancy of the Na3 site is incompatible with a proton bonded to the  
 203 O3x anion site at the  $\text{PO}_4$  group at P1x site (see Cámara *et al.* 2006 for a discussion of local  
 204 ordering). Although Raman spectrum does not show a clear indication of a deprotonation of  
 205 the  $\text{PO}_4$  group, there are other evidences from crystal data that supports this site assignment  
 206 (see below). The ideal, fully ordered end-member formula of fluorarrojadite-(BaNa) is  
 207  $\text{A}^1\text{Ba}^{\text{A}2}\text{B}^1\text{Na}^{\text{B}2}\text{Na}^{\text{Ca}}\text{Ca}^{\text{Na}1}\text{Na}^{\text{Na}2}\text{Na}^{\text{Na}3}\text{M}^{\text{Fe}}\text{Fe}_{13}\text{Al}(\text{PO}_4)_{11}(\text{PO}_3\text{OH})^W(\text{F}_{1.54}\text{OH}_{0.46})$ , which can be simplified  
 208 as  $\text{BaNa}_4\text{CaFe}_{13}\text{Al}(\text{PO}_4)_{11}(\text{PO}_3\text{OH})\text{F}_2$ , and requires  $\text{Na}_2\text{O}$  5.63,  $\text{BaO}$  6.97,  $\text{CaO}$  2.55,  $\text{FeO}$   
 209 42.44,  $\text{Al}_2\text{O}_3$  2.32,  $\text{P}_2\text{O}_5$  38.69,  $\text{F}$  1.73,  $\text{H}_2\text{O}$  0.41,  $\text{O}=\text{F}$  -0.73, total 100.00 wt.%. Studied  
 210 holotype material was homogenous, but some of earlier collected samples from Gemerská  
 211 Poloma studied by Števkó *et al.* (2015) suggest that a complete solid solution exists between  
 212 fluorarrojadite-(BaNa) and arrojadite-(BaNa), following a simple  $\text{F}^- \leftrightarrow (\text{OH})^-$  substitution.  
 213 Likewise, a solid solution exists between fluorarrojadite-(BaNa) and an as yet unapproved  
 214 new member of arrojadite group “fluordickinsonite-(BaNa)”.

## 215 X-ray diffraction data

216 Single-crystal X-ray studies of fluorarrojadite-(BaNa) were not carried out because of  
 217 the absence of suitable single crystals: as studied material is very fine grained (individual  
 218 grains up to 0.01 mm) and several attempts to obtain suitable single crystal from the fine  
 219 grained mass of fluorarrojadite-(BaNa) were unsuccessful.

220 X-ray powder diffraction data of fluorarrojadite-(BaNa) were recorded using a Bruker  
 221 D8 Advance diffractometer equipped with solid-state LynxEye detector and secondary

222 monochromator producing CuK $\alpha$  radiation housed at the Department of Mineralogy and  
223 Petrology, National Museum, Prague, Czech Republic. The instrument was operating at 40  
224 kV and 40 mA. In order to minimize the background, the powdered sample was placed on the  
225 surface of a flat silicon wafer in ethanol suspension. The powder pattern was collected in the  
226 Bragg–Brentano geometry in the range 3–75° 2 $\theta$ , step 0.01° and counting time of 30 s per step  
227 (total duration of experiment was ca. 3 days). Positions and intensities of diffractions were  
228 found and refined using the Pearson VII profile-shape function of the ZDS program package  
229 (Ondruš, 1993) and the unit-cell parameters were refined by the least-squares program of  
230 Burnham (1962). The X-ray powder diffraction data of fluorarrojadite-(BaNa) are given in  
231 **Table 3**. Unit-cell parameters of fluorarrojadite-(BaNa) refined for the monoclinic space  
232 group *Cc* are:  $a = 16.563(1)$  Å,  $b = 10.0476(6)$  Å,  $c = 24.569(1)$  Å,  $\beta = 105.452(4)^\circ$ ,  $V =$   
233  $3957.5(4)$  Å<sup>3</sup> and  $Z = 4$ . Application of Rietveld refinement is highly questionable considering  
234 that the structure has > 90 independent atom sites. However, we conducted a test using the  
235 collected data and the model published by Cámara *et al.* (2006) for arrojadite-(SrFe), allowing  
236 for refinement of cation occupancies at M1, A2, B1, Na3 and Ca sites (Ba vs. K, Na, Na vs.  
237 Fe, Na, Na and Ca vs. Sr, respectively). The chemistry at the M1 and M3 sites was allowed to  
238 vary, while was hold fixed in all the other M sites. The atom coordinates of every cation and  
239 anion sites in the structure were kept fixed. Refinement was performed with GSAS+EXPGUI  
240 software (Larson and Von Dreele, 1994; Toby, 2001). The residuals improved sensibly ( $wRp$   
241  $= 0.0398$ ,  $wRp$  after background subtraction 0.0911;  $R(F^2) = 0.1475$ ) when chemistry was  
242 allowed to vary in the above reported sites. Obviously, the results should interpreted with  
243 caution. Nevertheless the trend agrees well with what was expected from the formula obtained  
244 on the basis of crystal chemical criteria. Occupancy at M1 was found 18.0(7) eps, as expected  
245 for fractionation of Li at this site already found in dickinsonite-(KMnNa) by Cámara *et al.*  
246 (2006). Zn seems to order in M3 site that is among the smaller octahedra but yielded 29.1(6)

247 eps, evidently overestimated. The most interesting results are obtained for alkali sites: 48.5(4)  
248 vs. 43.1 eps from chemical formula in A1 site; 2.5(8) vs. 3.9 eps from chemical formula in A2  
249 site; 25.7(5) vs. 26.3 eps from chemical formula in Ca site; 2.5(8) vs. 3.9 eps from chemical  
250 formula in A2 site; 22.8(6) vs. 17.9 eps from chemical formula in B1 site; and 1.2(7) vs. 5.1  
251 eps from chemical formula in Na3 site. Therefore the worst agreement are found in the B1  
252 and Na3 sites, which are usually split sites (see Cámara *et al.* 2006) thus seriously challenging  
253 any plausible satisfactory result. **Figure 3** reports the observed and calculated pattern and the  
254 relative residuals. The results are a reasonable support of the proposed crystal chemical  
255 formula.

256

257

#### 258 **Relationship to the known species and origin**

259 As was mentioned, fluorarrojadite-(BaNa) is a member of the arrojadite group  
260 (Cámara *et al.*, 2006; Chopin *et al.*, 2005). Its existence was already noted in samples of  
261 fluoarrojadite-(BaFe) from the Sidabou-Kricha pegmatite in Morocco by Chopin *et al.* (2006)  
262 and it was also described as a product of the hydrothermal alteration of triphylite from the  
263 Nanping No. 31 granitic pegmatite in Fujian Province, China by Rao *et al.* (2014). The  
264 studied sample has a rather high content of Mn<sup>2+</sup>, among the highest reported for arrojadites  
265 in literature. Only the sample from Buranga (Rwanda) (von Knorring, 1969) has an higher  
266 Mn content and such it is very close to be classified as dickinsonite. It is not surprising that in  
267 the same locality (Gemerská Poloma) some minute crystals showed compositions classifiable  
268 as “fluordickinsonite-(BaNa)” (Števko *et al.*, 2015). The Mg content is fairly low (only 0.12  
269 *apfu*), lower than in most of the analyses reported for arrojadites, except for arrojadite-(PbFe)  
270 coming from Sapucaia (Moore and Ito, 1979) which contains 3.49 *apfu* of Mg and for  
271 arrojadite-(BaFe) from Spluga (Demartin *et al.*, 1996) which reaches 5.54 *apfu* of Mg, but

272 still far from being classifiable as carmoite-(BaFe). Another interesting chemical feature is the  
273 presence of significant Li (0.37 *apfu*), not uncommon in arrojadites although far lower than  
274 the amount present in arrojadite-(PbFe) from Sapucaia (0.86 *apfu*, data from Cámara *et al.*,  
275 2006).

276 In the Strunz mineral classification system fluorarrojadite-(BaNa) fits in subdivision  
277 8.BF: phosphates, arsenates, vanadates with additional anions, without H<sub>2</sub>O, with medium-  
278 sized and large cations and (OH, etc.):RO<sub>4</sub> < 0.5:1 (Strunz and Nickel, 2001). The comparison  
279 of physical properties of the valid mineral species of the arrojadite subgroup are given in  
280 [Table 4](#). The observed lattice parameters are among the largest of the arrojadite subgroup and  
281 this is due to the fairly low Mg content. In general, all the cell dimensions are negatively  
282 correlated with the Mg content. The value observed for the  $\beta$  angle deviates from the positive  
283 trend observed by Cámara *et al.* (2006), which compares the value of the  $\beta$  angle with the  
284 (Na+K) content (see their Fig. 1), for samples with vacant Na<sub>3</sub> site. This indication is in  
285 support of the presence of Na at the Na<sup>2</sup> site as suggested by the site assignment on the basis  
286 of crystal-chemical criteria and the weak evidence from Rietveld refinement of the presence  
287 of some occupation at this site.

288

289 Fluorarrojadite-(BaNa) and associated phosphates in quartz veins were formed from  
290 late-magmatic to early-hydrothermal P- and F-rich fluids, related to the adjacent granite.  
291 These relatively high-temperature fluids altered primary magmatic minerals of the granite  
292 (especially albite, K-feldspar, Li-rich micas and fluorapatite) and liberated elements (such as  
293 Na, K, Fe, Mn, Ca, Ba, Sr, and P) necessary for precipitation of the phosphate minerals.

294

295 **Acknowledgements:** The helpful comments of Jakub Plášil, Peter Leverett and Christian  
296 Chopin are greatly appreciated. Pavel Škácha is acknowledged for photography. FC thanks

297 Marco Merlini (Università di Milano, Italy) for help with GSAS-EXPGUI. This study was  
298 financially supported by the Ministry of Culture of the Czech Republic (DKRVO 2017/02;  
299 National Museum 00023272), by the Slovak Research and Development Agency under the  
300 APVV-14-0278 project, and by the Ministry of Education, Slovak Republic, the VEGA-  
301 1/0499/16 project.

302

### 303 **References**

- 304 Bajanič, Š., Ivanička, J., Mello, J., Pristaš, J., Reichwalder, P., Snopko, I., Vozár, J. and  
305 Vozárová, A. (1984) Geological map of the Slovenské Rudohorie Mts. - eastern part 1:  
306 50 000. Dionýz Štúr Institute of Geology, Bratislava.
- 307 Breiter, K., Broska, I. and Uher, P. (2015) Intensive low-temperature tectono-hydrothermal  
308 overprint of peraluminous rare-metal granite: a case study from the Dlhá dolina valley  
309 (Gemericum, Slovakia). *Geologica Carpathica* **63**, 19–36.
- 310 Burnham, C. W. (1962) Lattice constant refinement. *Carnegie Institute Washington Yearbook*  
311 **61**, 132–135.
- 312 Cámara, F., Oberti, R., Chopin, C. and Medenbach, O. (2006) The arrojadite enigma: I. A  
313 new formula and a new model for the arrojadite structure. *American Mineralogist*, **91**,  
314 1249–1259.
- 315 Cámara, F., Bravarolo, E., Ciriotti, M.E., Nestola, F., Radica, F., and Bracco, R. (2015)  
316 Fluorcarnoite-(BaNa), IMA 2015-062. CNMNC Newsletter No. 27, October 2015,  
317 1229. *Mineralogical Magazine* **79**, 1229–1236.
- 318 Chopin, C., Oberti, R. and Cámara, F. (2006) The arrojadite enigma: II. Compositional space,  
319 new members, and nomenclature of the group. *American Mineralogist*, **91**, 1260–1270.

- 320 Della Ventura, G., Bellatreccia, F., Radica, F., Chopin, C. and Oberti, R. (2014) The  
321 arrojadite enigma III. The incorporation of volatiles: a polarised FTIR spectroscopy  
322 study. *European Journal of Mineralogy*, **26**, 679–688.
- 323 Demartin, F., Gramaccioli, C. M., Pilati, T., and Sciesa, E. (1996) Sigismundite,  
324  $(\text{Ba,K,Pb})\text{Na}_3(\text{Ca,Sr})(\text{Fe,Mg,Mn})_{14}\text{Al}(\text{OH})_2(\text{PO}_4)_{12}$ , a new Ba-rich member of the  
325 arrojadite group from Spluga Valley, Italy. *Canadian Mineralogist*, **34**, 827–834.
- 326 Dianiška, I., Breiter, K., Broska, I., Kubiš, M. and Malachovský, P. (2002) First, high- $\text{K}$ , low- $\text{Al}_2\text{O}_3$ -  
327 rich Nb-Ta-Sn-specialised granite from the Carpathians - Dlhá dolina valley granite  
328 pluton, Gemeric superunit. *Geologica Carpathica*, **53**, Special Issue (CD-ROM).
- 329 Dianiška, I., Uher, P., Hurai, V., Huraiová, M., Frank, W., Konečný, F. and Král, J. (2007)  
330 Mineralization of rare-metal granites. Pp. 254-330. In: Hurai, V., ed. (2007) Sources of  
331 fluids and origin of mineralizations in the Gemeric unit. Open file report, Dionýz Štúr  
332 Institute of Geology, Bratislava (in Slovak).
- 333 Frost, R. L., Xi, Y., Schol, R. and Campos Horta, L. F. (2013) The phosphate mineral  
334 arrojadite-(KFe) and its spectroscopic characterization. *Spectrochimica Acta Part A:*  
335 *Molecular and Biomolecular Spectroscopy*, **109**, 138–145.
- 336 Kilík, J. (1997) Geological characteristic of the talc deposit in Gemerská Poloma-Dlhá dolina.  
337 *Acta Montanistica Slovaca*, **2**, 71–80 (in Slovak).
- 338 Kohút, M. and Štejn, H. (2005) Re-Os molybdenite dating of granite-related Sn-W-Mo  
339 mineralisation at Hnilec, Gemeric Superunit, Slovakia. *Mineralogy and Petrology* **85**,  
340 117–129.
- 341 Kubiš, M. and Broska, I. (2005) The role of boron and fluorine in evolved granitic rock  
342 systems (on the example of the Hnilec area, Western Carpathians). *Geologica*  
343 *Carpathica*, **56**, 193–204.

- 344 Kubiš, M. and Broska, I. (2010) The granite system near Betliar village (Gemic Superunit,  
345 Western Carpathians): evolution of a composite silicic reservoir. *Journal of*  
346 *Geosciences*, **55**, 131–148.
- 347 Lafuente, B., Downs, R.T., Yang, H. and Stone, N. (2015) The power of databases: the  
348 RRUFF project. In: Armbruster, T. and Danisi, R.M., eds. (2015) Highlights in  
349 Mineralogical Crystallography. De Gruyter, Berlin, 1–30.
- 350 Larson, A.C. and Von Dreele, R.B. (1994) General Structure Analysis System (GSAS) Los  
351 Alamos National Laboratory Report LAUR 86-748. Moore, P.B. and Ito, J. (1979)  
352 Alluaudites, wylieites, arrojadites: crystal chemistry and nomenclature. *Mineralogical*  
353 *Magazine*, **43**, 227–235.
- 354 Nakamoto, K. (1986) *Infrared and Raman Spectra of Inorganic and Coordination*  
355 *Compounds*. J. Wiley and Sons, New York.
- 356 Ondruš, P. (1993) A computer program for analysis of X-ray powder diffraction patterns.  
357 *Materials Sci. Forum, EPDIC-2, Fachea*, **133-136**, 297–300.
- 358 Petrasová, K., Faryad, S.W., Jeřábek, P. and Žáčková, E. (2007) Origin and metamorphic  
359 evolution of magnesian talc and adjacent rocks near Gemerská Poloma, Slovak  
360 Republic. *Journal of Geosciences*, **52**, 125–132.
- 361 Petřík, I. and Kohút, M. (1997) The evolution of granitoid magmatism during the Hercynian  
362 orogen in the Western Carpathians. In Geological Evolution of the Western Carpathians  
363 (Grecula, P., Hovorka, D. and Putiš, M. eds.). *Mineralia Slovaca*, Monographic Series,  
364 235–252.
- 365 Petřík, I., Čík, Š., Miglierini, M., Vaculovič, T., Dianiška, I. and Ozdín, D. (2014) Alpine  
366 oxidation of lithium micas in Permian S-type granites (Gemic unit, Western  
367 Carpathians, Slovakia). *Mineralogical Magazine*, **78**, 507–533.

- 368 Poller, U., Uher, P., Broska, I., Plašienka, D. and Janák, M. (2002) First Permian - Early  
369 Triassic zircon ages for tin-bearing granites from the Gemeric Unit (Western  
370 Carpathians, Slovakia): connection to the post-collisional extension of the Variscan  
371 orogen and S-type granite magmatism. *Terra Nova* **14**, 41–48.
- 372 Pouchou, J. L. and Pichoir, F. (1991) Quantitative analysis of homogeneous or stratified  
373 microvolumes applying the model "PAP." In: Heinrich, K.F.J. and Newbury, D.E. (eds)  
374 *Electron Probe Quantitation*. Plenum Press, New York, 31–75.
- 375 Rao, C., Wang, R.C., Hatert, F. and Baijot, M. (2014) Hydrothermal transformations of  
376 triphylite from the Nanping No. 31 pegmatite dyke, southern China. *European*  
377 *Journal of Mineralogy*, **26**, 179–188.
- 378 Števkó, M., Uher, P., Sejkora, J., Malíková, R., Škoda, P. and Vaculovič, T. (2015) Phosphate  
379 minerals from the hydrothermal quartz veins in specialized S-type granites, Gemerská  
380 Poloma (Western Carpathians, Slovakia). *Journal of Geosciences*, **60**, 237–249.
- 381 Strunz, H. and Nickel, E.H. (2001) Strunz mineralogical tables. Chemical Structural mineral  
382 classification system. 9<sup>th</sup> edition. E. Schweizerbart'sche Verlagsbuchhandlung (Nägele u.  
383 Obermiller), Stuttgart, 876 pp.
- 384 Toby, B.H. (2001) EXPGUI, a graphical user interface for GSAS. *Journal of Applied*  
385 *Crystallography*, **34**, 210–213.
- 386 Uher, P. and Broska, I. (1996) Post-orogenic Permian granitic rocks in the Western  
387 Carpathian–Pannonian area: geochemistry, mineralogy and evolution. *Geologica*  
388 *Carpathica*, **47**, 311–321.
- 389 Vignola, P., Hatert, F., Baijot, M., Dal Bo, F., Andò, S., Bersani, D., Risplendente, A. and  
390 Vanini, F. (2015) Arrojadite-(BaNa), IMA 2014-071. CNMNC Newsletter No. 23,  
391 February 2015, page 55; *Mineralogical Magazine*, **79**, 51–58.



392 von Knorring, O. (1969) A note on the phosphate mineralisation at the Buranga pegmatite,  
393 Rwanda. *Bulletin du Service géologique du Rwanda*, **5**, 42–45.  
394

Prepublished Article



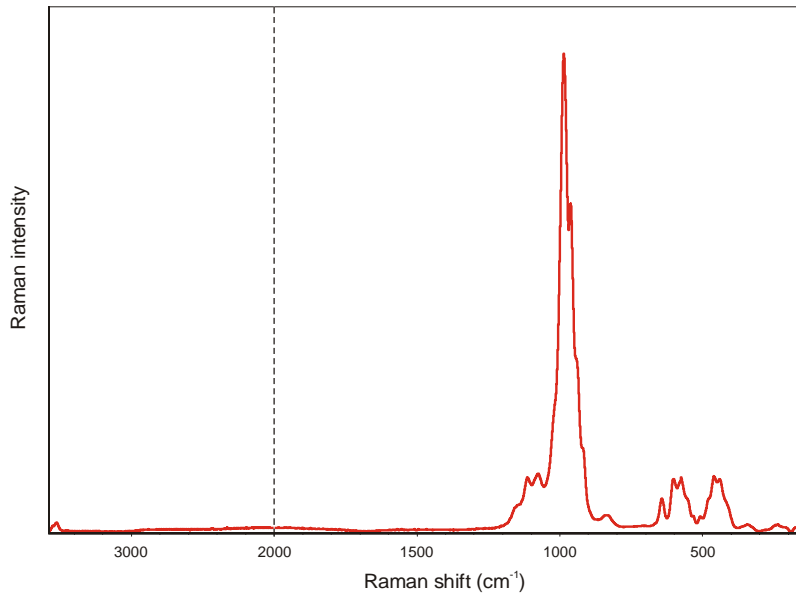
396

397 Fig. 1. Yellowish-brown fine grained aggregate of fluoroarjadite-(BaNa) associated with  
398 minor dark green grains of fluorapatite in quartz matrix. Field of view is 40 mm.

399 Photographed by Pavel Škafář.

400

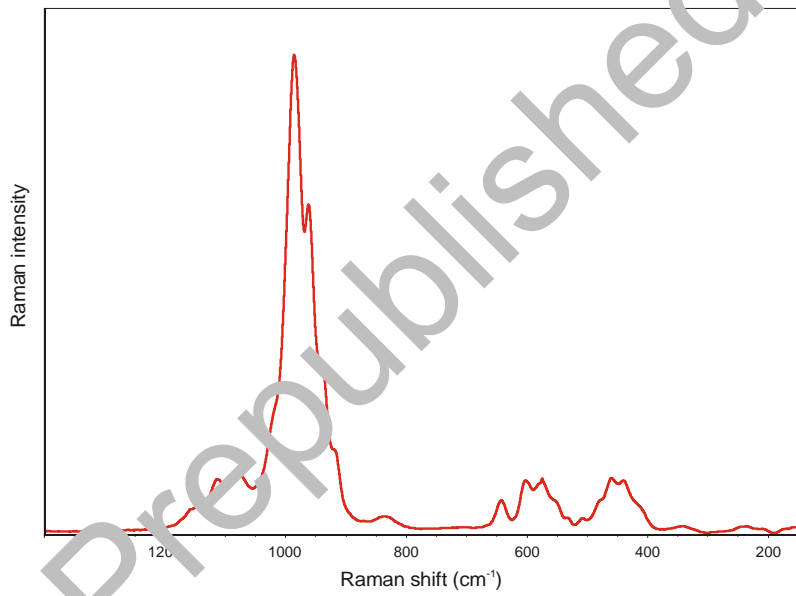
Prepublished Article



401

402 Fig. 2a. Raman spectrum of fluorarrojadite-(BaNa) from Gemerská Poloma, full range.

403

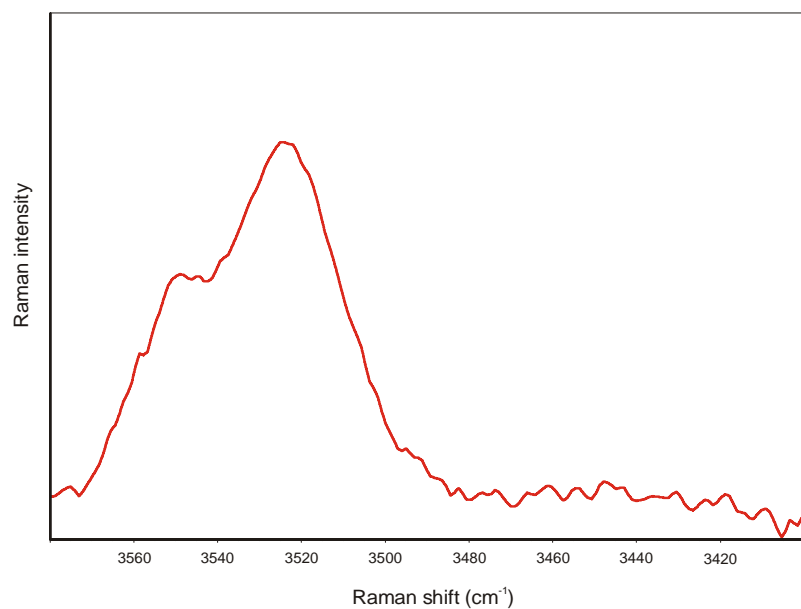


404

405 Fig. 2b. Raman spectrum of fluorarrojadite-(BaNa) from Gemerská Poloma, range 150 – 1400

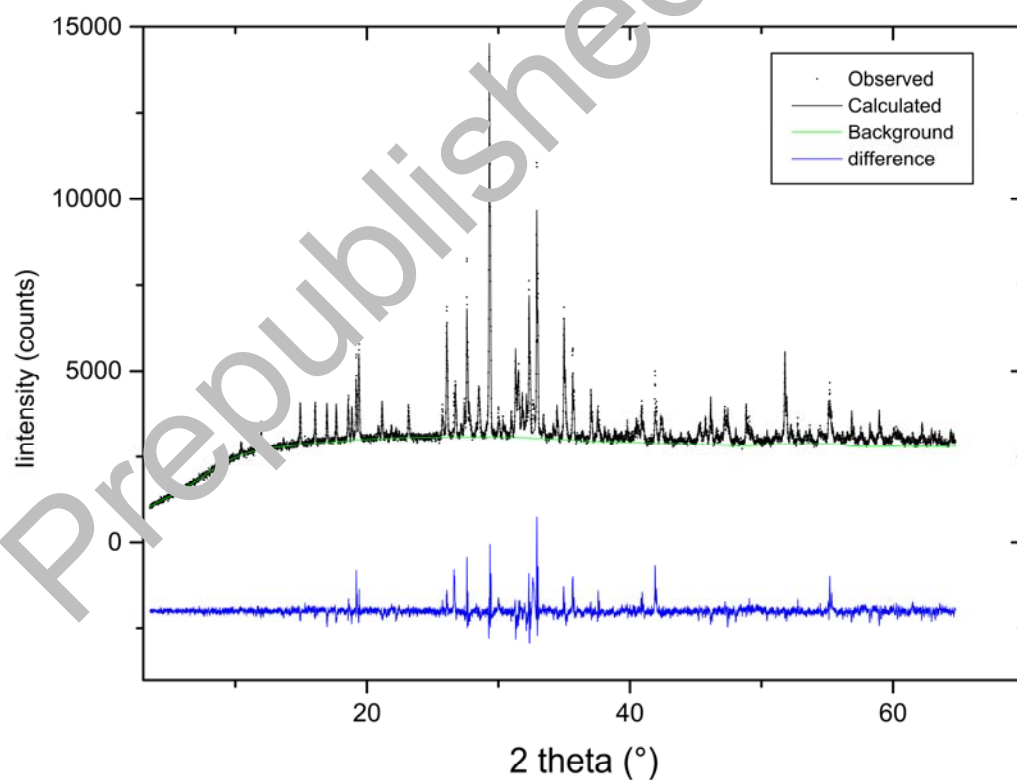
406  $\text{cm}^{-1}$ .

407



408

409 Fig. 2c. Raman spectrum of fluorarrojadite-(BaNa) from Gemerkő, Romania, range 3400 –  
 410 3580  $\text{cm}^{-1}$ .



411

412 Figure 3. Observed powder pattern of fluorarrojadite-(BaNa). The calculated intensities,  
 413 subtracted background and residuals obtained by Rietveld refinement (see text) are also

Prepublished Article

Table 1. Chemical composition (in wt%) of fluorarrojadite-(BaNa).

Constituent	Mean	Range	SD	Standard
K <sub>2</sub> O	0.76	0.70 - 0.86	0.07	sanidine
Na <sub>2</sub> O	5.72	5.52 - 5.84	0.36	albite
Li <sub>2</sub> O*	0.26	0.26		NIST SRM 610
BaO	4.91	4.02 - 5.73	0.18	baryte
SrO	0.98	0.70 - 1.36	0.18	SrSO <sub>4</sub>
CaO	1.93	1.85 - 2.01	0.08	fluorapatite
PbO	0.23	0.12 - 0.38	0.12	vanadinite
MgO	0.23	0.21 - 0.24	0.03	Mg <sub>2</sub> SiO <sub>4</sub>
ZnO	0.22	0.19 - 0.24	0.11	gahnite
MnO	17.08	16.86 - 17.32	0.46	spessartine
FeO	25.51	25.21 - 26.15	0.55	almandine
Al <sub>2</sub> O <sub>3</sub>	2.43	2.31 - 2.50	0.09	sanidine
Sc <sub>2</sub> O <sub>3</sub> *	0.26	0.26		NIST SRM 610
Ga <sub>2</sub> O <sub>3</sub> *	0.08	0.08		NIST SRM 610
TiO <sub>2</sub>	0.07	0.05 - 0.10	0.02	titanite
P <sub>2</sub> O <sub>5</sub>	39.75	39.21 - 40.26	0.5	fluorapatite
F	1.36	1.30 - 1.46	0.11	topaz
H <sub>2</sub> O**	0.47			
O=F	-0.57			
Total	101.67			

\* obtained by LA-ICP-MS

\*\* calculated as  $(F+OH+Na3) = 3 \text{ apfu}$

Table 3. X-ray powder diffraction data of fluorarrojadite-(BaNa) from Gemerská Poloma; the strongest diffractions are reported in bold.

$I_{meas.}$	$d_{meas.}$	$d_{calc.}$	$h$	$k$	$l$	$I_{meas.}$	$d_{meas.}$	$d_{calc.}$	$h$	$k$	$l$	$I_{meas.}$	$d_{meas.}$	$d_{calc.}$	$h$	$k$	$l$
1	8.506	8.504	1	1	0	12	2.5959	2.5965	1	3	-6	9	1.7577	1.7579	6	4	2
2	7.638	7.634	2	0	-2	<b>33</b>	<b>2.5563</b>	<b>2.5583</b>	<b>0</b>	<b>2</b>	<b>8</b>	4	1.7551	1.7563	8	0	4
3	7.436	7.433	1	1	-2	<b>33</b>	<b>2.5563</b>	<b>2.5558</b>	<b>4</b>	<b>2</b>	<b>4</b>	4	1.7551	1.7551	7	1	6
1	6.494	6.495	1	1	2	8	2.5447	2.5446	6	0	-6	3	1.7287	1.7288	6	2	-12
5	5.940	5.945	0	0	4	<b>23</b>	<b>2.5117</b>	<b>2.5119</b>	<b>0</b>	<b>4</b>	<b>0</b>	1	1.7149	1.7146	3	5	-7
4	5.527	5.524	2	0	-4	5	2.4204	2.4202	4	2	-8	1	1.7135	1.7138	5	5	-1
5	5.235	5.233	1	1	-4	9	2.4181	2.4175	6	2	-2	1	1.7135	1.7130	1	1	-14
6	5.023	5.024	0	2	0	7	2.3875	2.3870	6	2	-4	2	1.7104	1.7099	4	4	-10
7	4.775	4.774	3	1	-2	2	2.3570	2.3570	3	1	-10	4	1.7008	1.7008	5	1	0
5	4.704	4.703	3	1	0	3	2.3377	2.3375	6	2	-5	3	1.6819	1.6819	1	5	2
11	4.627	4.628	0	2	2	1	2.3118	2.3111	5	3	0	2	1.6788	1.6787	5	1	10
14	4.577	4.578	1	1	4	1	2.2970	2.2970	1	3	7	2	1.6749	1.6750	5	2	8
2	4.253	4.252	2	2	0	1	2.2641	2.2635	4	2	-9	8	1.6606	1.6607	3	5	-8
5	4.198	4.200	3	1	-4	3	2.2568	2.2565	5	3	-5	8	1.6606	1.6605	2	2	-14
1	4.196	4.197	2	2	-2	8	2.1985	2.1983	7	1	-6	3	1.6587	1.6582	0	6	2
1	4.128	4.130	4	0	-2	5	2.1494	2.1494	0	2	10	3	1.6552	1.6579	8	2	4
2	4.058	4.059	3	1	2	4	2.1458	2.1461	4	4	-2	5	1.6557	1.6563	1	3	12
1	3.962	3.963	0	0	6	5	2.1268	2.1260	4	4	0	2	1.6308	1.6310	1	5	8
6	3.837	3.837	0	2	4	3	2.1218	2.1217	0	4	6	1	1.6223	1.6222	3	1	-15
6	3.837	3.835	2	2	2	3	2.0910	2.0906	7	1	2	4	1.6223	1.6222	1	1	14
1	3.542	3.544	2	2	3	2	2.0554	2.0549	7	1	2	8	1.6124	1.6124	4	0	12
1	3.512	3.513	4	0	2	3	2.0295	2.0296	5	2	4	2	1.5939	1.5944	10	0	-8
5	3.457	3.458	3	1	-6	7	1.9942	1.9958	8	0	0	2	1.5939	1.5936	7	1	8
5	3.457	3.454	0	2	5	8	1.9770	1.9771	5	-2		5	1.5770	1.5770	6	0	10
<b>21</b>	<b>3.412</b>	<b>3.412</b>	<b>1</b>	<b>1</b>	<b>6</b>	11	1.9601	1.9606	2	2	10	2	1.5615	1.5626	8	4	0
12	3.328	3.328	3	1	4	1	1.9601	1.9597	4	2	8	3	1.5596	1.5602	8	2	-12
2	3.277	3.278	1	3	0	3	1.9429	1.9428	2	4	-8	3	1.5596	1.5589	10	2	-6
2	3.271	3.271	1	3	-1	1	1.9288	1.9287	7	3	-2	6	1.5336	1.5335	4	6	-4
6	3.247	3.248	2	2	4	2	1.9255	1.9258	7	1	4	2	1.5268	1.5269	7	5	-4
<b>37</b>	<b>3.224</b>	<b>3.225</b>	<b>2</b>	<b>0</b>	<b>8</b>	3	1.9204	1.9201	3	3	8	2	1.5268	1.5268	10	0	-10
8	3.205	3.205	1	3	2	3	1.9190	1.9186	0	4	8	1	1.5197	1.5197	10	2	-8
10	3.126	3.129	2	2	-6	4	1.9180	1.9176	4	4	4	1	1.5197	1.5196	8	4	-8
10	3.126	3.124	3	1	-7	8	1.9086	1.9085	8	0	-8	4	1.4863	1.4866	5	5	-10
<b>100</b>	<b>3.090</b>	<b>3.090</b>	<b>4</b>	<b>2</b>	<b>-4</b>	3	1.8852	1.8852	7	3	0	4	1.4863	1.4862	2	6	6
5	2.972	2.9726	0	0	8	7	1.8580	1.8583	4	4	-8	3	1.4698	1.4703	9	1	-13
3	2.9386	2.9391	1	3	-4	7	1.8580	1.8571	6	4	-2	3	1.4698	1.4691	11	1	-7
1	2.9226	2.9216	5	1	-5	1	1.8436	1.8443	5	3	-10	3	1.4698	1.4694	2	2	-16
4	2.8791	2.8788	4	2	2	1	1.8436	1.8431	6	4	-4	3	1.4638	1.4633	10	2	2
<b>22</b>	<b>2.8499</b>	<b>2.8499</b>	<b>3</b>	<b>3</b>	<b>-2</b>	2	1.8428	1.8429	1	1	-13	2	1.4589	1.4590	0	6	8
18	2.8327	2.8346	3	3	0	2	1.8428	1.8412	6	0	-12	2	1.4589	1.4585	4	6	4
1	2.8308	2.8312	3	1	-8	1	1.8265	1.8277	7	3	-7	2	1.4411	1.4411	2	4	-14
11	2.8062	2.8064	1	3	4	1	1.8265	1.8266	6	4	0	2	1.4318	1.4318	4	0	14
9	2.7782	2.7778	5	1	-6	3	1.8019	1.8017	7	3	2	2	1.4294	1.4295	1	5	-12
17	2.7619	2.7618	4	0	-8	2	1.7799	1.7799	9	1	-6	2	1.4294	1.4295	4	4	-14
11	2.7580	2.7579	6	0	-2	2	1.7799	1.7795	8	0	-10	5	1.4253	1.4250	6	6	-4
<b>56</b>	<b>2.7135</b>	<b>2.7138</b>	<b>2</b>	<b>2</b>	<b>6</b>	1	1.7721	1.7718	4	4	6	5	1.4253	1.4252	0	2	16
5	2.6732	2.6733	3	3	2	14	1.7596	1.7596	2	4	-10	4	1.4236	1.4235	8	2	8
3	2.6166	2.6165	2	2	-8	14	1.7596	1.7594	2	0	-14	1	1.4145	1.4156	6	2	-16

Table 2. Trace element LA-ICP-MS analyses of fluorarrodite-(BaNa) from Gemerská Poloma (in ppm).

Spot #	1	2	3	4	5	6	7	8	9	10	11	12	13	14	15	Average	Det. limit
Li	1178	1204	1203	1347	1200	1076	1106	1424	1293	1283	1155	1081	209	1143	942	1189	0.2
Be	2.2	2.9	2.2	3.5	2.5	1.9	2.6	2.3	2.2	2.1	3.9	3.0	2.5	3.1	2.3	2.6	0.1
B	10	9.0	8.5	10	9.3	6.7	8.2	12	6.5	6.0	5.7	5.7	5.5	6.5	4.8	7.7	1.6
Sc	1458	1384	1483	1150	1146	1885	1656	2183	1754	1741	1258	1472	1944	2081	1755	1623	0.2
Ti	299	367	337	328	310	285	273	360	339	302	292	292	336	315	284	314	0.4
V	<	<	<	<	<	<	<	<	<	<	<	<	<	<	<	<	0.1
Cr	1.4	<	1.3	1.9	0.6	<	<	1.0	<	<	2.4	0.6	<	<	<	1.3	0.3
Co	0.5	0.4	0.4	3.1	0.5	0.2	0.4	0.6	0.7	0.5	1.4	0.3	0.4	0.3	0.4	0.6	0.1
Cu	2.3	1.6	1.7	2.6	2.0	2.2	1.8	3.6	2.1	2.2	1.6	2.0	3.3	2.7	2.5	2.3	0.3
Ga	541	545	693	560	562	642	609	709	621	636	511	524	555	673	621	600	0.1
Ge	64	67	73	62	63	54	53	59	49	57	47	41	41	44	39	53	0.1
Rb	47	57	57	73	53	34	39	49	59	45	71	56	50	35	37	51	0.1
Y	14	19	17	19	17	11	14	16	17	14	17	17	14	16	14	16	0.1
Zr	0.7	0.9	0.7	1.0	0.8	0.6	0.8	0.9	0.8	0.6	0.9	0.8	0.8	0.6	0.7	0.8	0.1
Nb	0.7	1.1	0.4	0.6	0.6	0.6	0.6	0.8	0.8	0.5	0.5	0.5	0.6	1.2	0.9	0.7	0.1
Sn	3.0	0.4	<	<	<	<	<	<	<	<	<	0.2	<	2.1	1.1	1.4	0.1
Sb	0.5	0.5	0.5	0.9	0.7	0.5	0.4	0.5	0.5	0.7	0.5	0.5	0.5	0.9	0.5	0.6	0.1
La	1.8	1.1	1.2	1.1	1.0	0.8	0.9	1.0	1.0	1.0	0.7	0.9	0.9	0.8	0.8	1.0	0.1
Ce	4.8	2.8	3.3	3.5	3.2	2.1	2.7	2.8	2.7	2.5	2.5	2.2	2.3	2.3	2.2	2.8	0.1
Pr	<	<	<	<	<	<	<	<	<	<	<	<	<	<	<	<	0.1
Nd	1.3	0.8	1.0	1.3	1.2	0.5	0.8	1.0	0.9	0.6	0.6	0.6	0.7	0.7	0.5	0.8	0.1
Sm	0.5	0.3	0.5	0.4	0.4	0.3	0.7	0.6	0.4	0.4	0.2	0.3	0.3	0.3	0.4	0.4	0.1
Eu	3.5	2.9	3.5	3.2	3.2	2.8	2.5	3.6	2.8	3.3	2.6	2.8	3.1	3.1	3.1	3.1	0.1
Gd	0.6	0.4	0.6	0.7	0.6	0.3	0.5	0.7	0.5	0.4	0.5	0.4	0.5	0.5	0.5	0.5	0.1
Tb	<	<	<	<	<	<	<	<	<	<	<	<	<	<	<	<	0.1
Dy	1.4	1.6	1.8	1.6	1.8	1.3	1.3	1.8	1.8	1.3	1.6	1.6	1.5	1.4	1.4	1.5	0.1
Ho	<	<	<	<	<	<	<	<	<	<	<	<	<	<	<	<	0.1
Er	1.3	1.6	1.7	1.6	1.5	1.0	1.2	1.4	1.3	1.3	1.2	1.3	1.4	1.3	1.2	1.4	0.1
Tm	0.3	0.4	0.5	0.4	0.4	0.3	0.4	0.4	0.4	0.3	0.4	0.4	0.4	0.4	0.3	0.4	0.1
Yb	3.6	4.9	4.6	5.5	4.4	3.0	4.2	4.3	3.7	4.0	3.9	4.0	4.2	4.2	3.6	4.1	0.1
Lu	0.7	0.9	0.9	0.8	0.9	0.6	0.7	0.8	0.8	0.8	0.8	0.8	0.8	0.8	0.7	0.8	0.1
Th	<	<	<	<	<	<	<	<	<	<	<	<	<	<	<	<	0.1
U	1.1	1.4	1.1	1.9	1.3	1.1	1.3	1.8	0.8	0.8	1.5	1.3	0.9	1.8	1.1	1.3	0.1



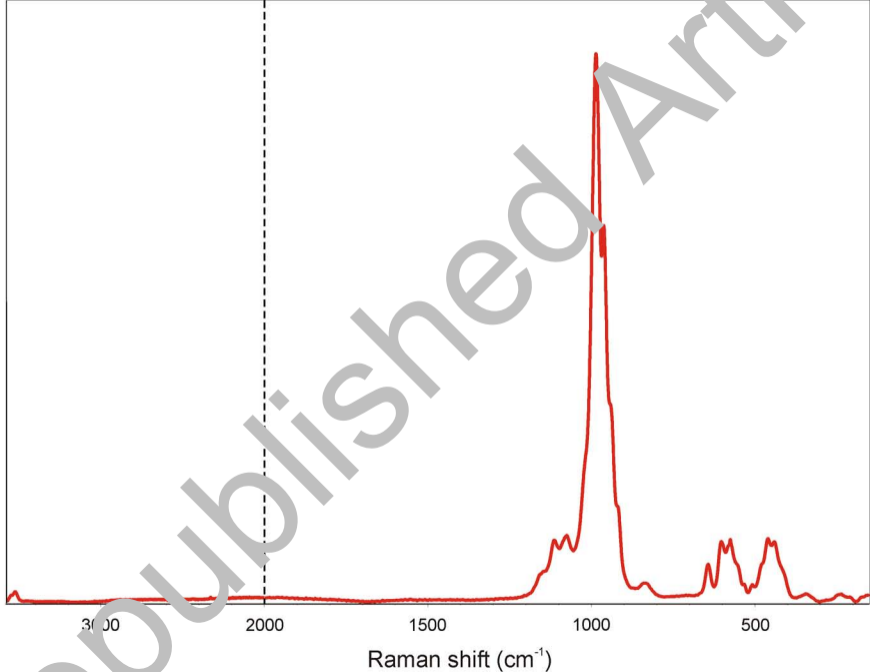
Table 4. Comparison of the physical properties for valid members of the arrojadite group (dickinsonites and fluorcarmoite-(BaNa) are not included).

mineral	fluorarrojadite-(BaNa)	fluorarrojadite-(BaFe)	arrojadite-(BaFe)	arrojadite-(KFe)	arrojadite-(KNa)	arrojadite-(PbFe)	arrojadite-(SrFe)	arrojadite-(BaNa)
type locality	Gemerská Poloma, Slovakia	Sidi Bou Kricha, Morocco	Spluga Valley, Italy	Nickel Plate Mine, USA	Rapid Creek, Canada	Sapucaia, Brazil	Horrsjöberg, Sweden	Luna, Dorio, Italy
reference	this work	Chopin <i>et al.</i> (2006)	Demartin <i>et al.</i> (1996), Chopin <i>et al.</i> (2006)	Chopin <i>et al.</i> (2006)	Cámara <i>et al.</i> (2006)	Chopin <i>et al.</i> (2006)	Cámara <i>et al.</i> (2006)	Vignola <i>et al.</i> (2015)
ideal formula	$(\text{Ba}\square)(\text{Na})_2\text{Ca}(\text{Na}_2\square)\text{Fe}_{13}\text{Al}(\text{PO}_4)_{11}(\text{PO}_3\text{OH})\text{F}_2$	$(\text{Ba}\square)(\text{Fe}^{2+}\square)\text{Ca}(\text{Na}_2\square)\text{Fe}_{13}\text{Al}(\text{PO}_4)_{11}(\text{PO}_3\text{OH})\text{F}_2$	$(\text{Ba}\square)(\text{Fe}^{2+}\square)\text{Ca}(\text{Na}_2\square)\text{Fe}_{13}\text{Al}(\text{PO}_4)_{11}(\text{PO}_3\text{OH})(\text{OH})_2$	$(\text{KNa})(\text{Fe}^{2+}\square)\text{Ca}(\text{Na}_2\square)\text{Fe}_{13}\text{Al}(\text{PO}_4)_{11}(\text{PO}_3\text{OH})(\text{OH})_2$	$(\text{KNa})(\text{Na})\text{Ca}(\text{Na}_2\square)\text{Fe}_{13}\text{Al}(\text{PO}_4)_{11}(\text{PO}_3\text{OH})\text{H}_2$	$(\text{Pb}\square)(\text{Fe}^{2+}\square)\text{Ca}(\text{Na}_2\square)\text{Fe}_{13}\text{Al}(\text{PO}_4)_{11}(\text{PO}_3\text{OH})(\text{OH})_2$	$(\text{Sr}\square)(\text{Fe}^{2+}\square)\text{Ca}(\text{Na}_2\square)\text{Fe}_{13}\text{Al}(\text{PO}_4)_{11}(\text{PO}_3\text{OH})(\text{OH})_2$	$\text{BaNa}_3(\text{NaCa})\text{Fe}_{13}\text{Al}(\text{PO}_4)_{11}(\text{PO}_3\text{OH})(\text{OH})_2$
crystal system	monoclinic	monoclinic	monoclinic	monoclinic	monoclinic	monoclinic	monoclinic	monoclinic
space group	<i>Cc</i>	<i>Cc</i>	<i>C2/c</i> or <i>Cc</i>	<i>Cc</i>	<i>Cc</i>	<i>Cc</i>	<i>Cc</i>	<i>C2/c</i>
<i>a</i> [Å]	16.563(1)	16.4970(9)	16.406(5)	no data	16.5220(11)	16.4304(9)	16.3992(7)	16.4984(6)
<i>b</i> [Å]	10.0476(6)	10.0176(5)	9.945(3)	no data	10.0529(7)	9.9745(5)	9.9400(4)	10.0228(3)
<i>c</i> [Å]	24.669(1)	24.6359(13)	24.470(5)	no data	24.6477(16)	24.5869(13)	24.4434(11)	24.648(1)
$\beta$ [°]	105.452(4)	105.649(2)	105.73(2)	no data	105.509(2)	105.485(2)	105.489(1)	105.850(4)
<i>V</i> [Å <sup>3</sup> ]	3957.5(4)	3920.42(5)	3843(2)	no data	3932.2(7)	3883.2(5)	3839.76(46)	3921
<i>Z</i>	4	4	4	no data	4	4	4	4
strongest powder X-ray diffractions	3.412/21 3.224/37 3.040/100 2.8499/22 2.7135/56 2.5563/33 2.5117/23	3.4003/31.2 3.2108/47.5 3.0319/100 2.8413/34.1 2.8285/30.0 2.7595/32.9 2.7031/68.5 2.5433/38.1	3.010/100* 3.178/51 2.678/42 2.523/27 2.805/25 2.775/21 2.741/21 2.732/21	no data	5.8614/28.8 5.0264/27.5 3.1857/33.5 3.0498/100 2.8529/22.4 2.7979/24.9 2.7933/28 2.7532/22.8 2.6908/71.3	4.5534/25.1 3.20882/43.1 3.0186/100 2.8291/35.0 2.8196/32.9 2.7496/29.1 2.6982/54.8 2.5376/30.4	3.3784/26.2 3.2931/21.0 3.1925/41.2 3.0093/100 2.8202/23.5 2.8053/28.4 2.7370/27.8 2.7304/20.1 2.6861/69.9	3.488/28 3.303/46 3.137/100 2.878/32 2.818/61 2.667/35
density	3.650 g.cm <sup>-3</sup>	3.650 g.cm <sup>-3</sup>	3.544 g.cm <sup>-3</sup>	no data	3.437 g.cm <sup>-3</sup>	3.596 g.cm <sup>-3</sup>	3.569 g.cm <sup>-3</sup>	3.76 g.cm <sup>-3</sup>
colour	yellowish-brown to greenish-yellow	dark yellowish-green	grayish green	dark yellowish-green	yellow	pale honey	green	pale grayish-green

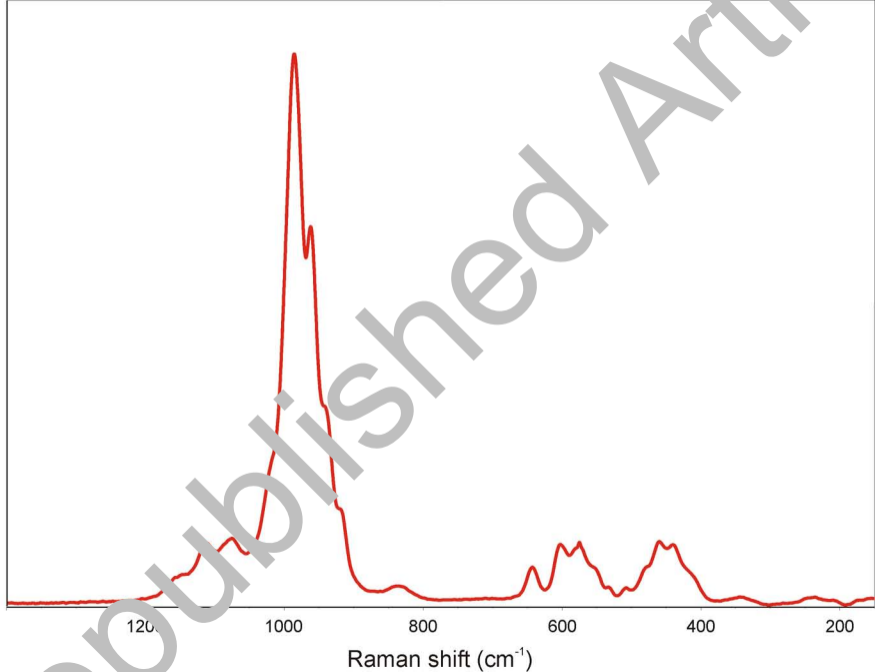
\* data from Demartin *et al.* (1996) for space group *C2/c*



Raman intensity



Raman intensity



1200

1000

800

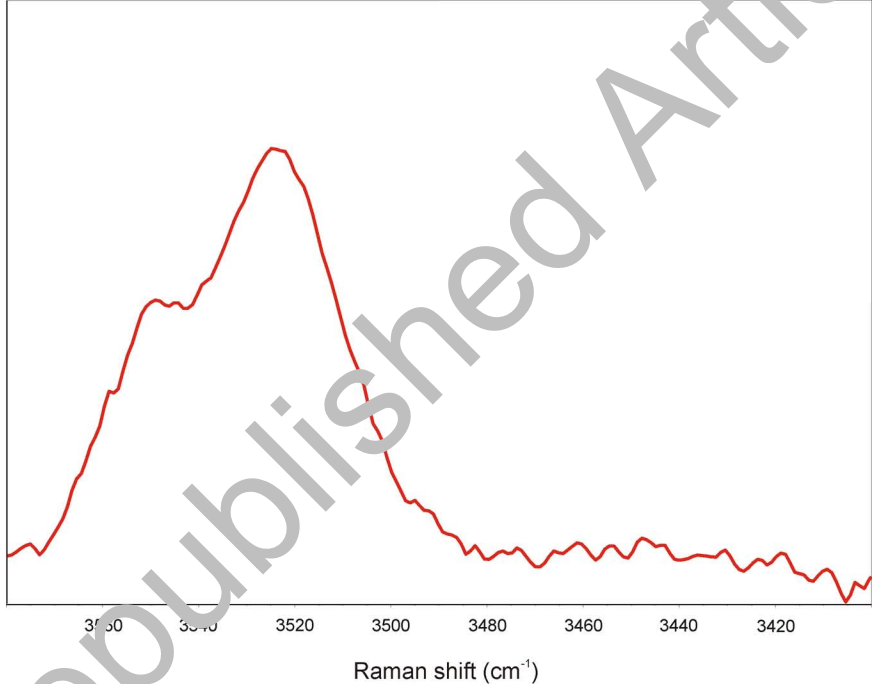
600

400

200

Raman shift ( $\text{cm}^{-1}$ )

Raman intensity



Raman shift (cm<sup>-1</sup>)

